IEEE Access
Multidisciplinary | Rapid Review | Open Access Journal

Received February 17, 2020, accepted February 25, 2020, date of publication March 3, 2020, date of current version March 12, 2020.

Digital Object Identifier 10.1109/ACCESS.2020.2977938

Robust Tracking for Small Target Groups With Dynamic Outlines

CHAO ZHOU[1], RUI WANG[1], AND CHENG HU[1,2]
[1]Radar Research Laboratory, School of Information and Electronics, Beijing Institute of Technology, Beijing 100081, China
[2]Key Laboratory of Electronic and Information Technology in Satellite Navigation, Ministry of Education, Beijing 100081, China

Corresponding author: Rui Wang (wangrui.bit@bit.edu.cn)

This work was supported in part by the National Natural Science Foundation of China Grant 31727901, and in part by the China Postdoctoral Science Foundation under Grant 2019M660486.

ABSTRACT Low altitude small target group has the special motion characteristics of orderly as a whole and flexibly as individuals. The performances of traditional target tracking algorithms (such as centroid tracking, geometric centre tracking, etc.) decrease obviously when the group outline changes. Hence in this paper, a robust tracking algorithm for target group with dynamic outline is studied. Aiming at the two key issues of group division and equivalent tracking point estimation, a robust group division algorithm, which can maintain the stability of group division results under any reference point selection, is firstly introduced. Then, on this basis, a new optimal tracking point estimation method is proposed by introducing the group structure into the likelihood function. The simulation results show that this proposed method can effectively improve the robustness of low altitude small target group tracking in the scene of group merging and group splitting.

INDEX TERMS Dynamic outlines, equivalent point estimation, group division, group tracking.

I. INTRODUCTION

Low altitude area, of which the altitude is less than 1km, has great value in applications of agriculture, medical treatment, transportation, etc [1], [2]. However, low altitude small target groups (LSTG) such as bird flocks and drone swarms have become non-ignorable security threats to this area. Due to their special motion characteristics (orderly as a whole and flexibly as individuals), existing technologies can hardly achieve ideal monitoring effects. Each year, these LSTG not only cause huge economic losses in civil aviation, but also may be maliciously used to endanger public safety [3], [4]. Therefore, it is particularly necessary to develop effective LSTG monitoring technologies.

Modern radar has been regarded as one of the most effective means to detect LSTG, because of its advantages of long detection range, high resolution and all-day/all-weather operation ability [5], [6]. There have been many researches on radar tracking algorithms for single and multiple targets situations [7]–[10]. However, the problem of tracking target groups with dynamic outlines has not been fully addressed.

The associate editor coordinating the review of this manuscript and approving it for publication was Wei Wang.

There are mainly three hot issues in the researches of radar target group tracking, which are group centre tracking, group outlines estimation and individual target tracking. This paper mainly discusses the first, which is the basis of the other two issues. Early researches mainly focused on formation group tracking. The basic idea is to take the target group as a whole and track the centre of the group, that is, the central group tracking (CGT) algorithm [11]. Afterwards, aiming at the problem of centre migration caused by miss detections and occlusions of group members, a formation group tracking (FGT) algorithm was proposed by Flad and Tenser [12]. The algorithm maintains the tracks of group centre and edges at the same time, thus achieving more robust performance through the mutual assistance of multiple tracks. In 1990, a general model, which divides the group tracking process into two aspects of centre tracking and outline tracking, was established in [13]. Since then, the research focus has gradually shifted to the latter, i.e., shape modelling of target group, and formed a number of valuable research results. For example, in [14], Granstrom and Orguner approximated the group outline as ellipses and introduced random matrix (RM) which obeys inverse Wishart distribution to represent the shape of objects. The motion state and extended state of the group are then estimated with Bayesian recursion method.

In [15], Amadou *et al.* modelled the measurements set with random finite sets (RFS) theory and estimated the group state with particle filtering method. In order to further improve the modelling accuracy of group outline, Baum and Hanebeck proposed a random hypersurface model (RHM) method [16]. The method assumes that the target measurements are generated from sources on the contour surface of the group, and describes the extended state of the group with measurement sources modelling. Furthermore, in order to model target groups with arbitrary outlines, the level set RHM method and multi-ellipse modelling method are proposed. By making use of the level set of given shape function for outline transformation, the former method can model any filled shape [17], while the latter converts the tracking problem of a non-elliptic target group into the problem of parameters estimation of multiple sub-ecliptics [18]. In addition, some filtering algorithms based on particle filtering and Monte Carlo methods are also used for state estimation of such targets. For example, in [19] Pang *et al.* expected to observe only ''small'' changes in group structure over short time intervals and proposed a Markov chain Monte Carlo (MCMC)-particles algorithm. In [20], Gning *et al.* used the evolutionary graph network model to describe the group structure, and used JPDA and particle filtering to realize track association and filtering, respectively.

These methods have achieved good performances in extended targets/formation group tracking [21]–[24], but they have two main problems when modelling group outlines of LSTG:

1) Current outline modelling methods are essentially proposed for extended targets and formation groups, which are generally rigid bodies. For this kind of targets, the outline change of measurements set is mainly due to the change of target posture, which is essentially different from the outline change of LSTG such as bird flocks and drone swarms. Therefore, the above models cannot achieve ideal performance in describing the outline characteristics of LSTG.
2) In the researches of outline modelling, the centroid point is usually used to describe the motion of the whole group, and on this basis, the interaction between centroid point and group outline is established. However, for different target groups or different detection requirements, whether the centroid point can be used as the optimal description of the whole motion of the target group is still a problem to be studied.

In order to distinguish from the centroid point mentioned in existing literatures, in this paper, the point reflecting the whole moving state of a target group is called the equivalent tracking point (equivalent point for short). The selection of the equivalent points is directly related to the tracking performance, on the other hand, it is closely related to the outline modelling of target groups, hence is the basis and core of target group tracking.

Therefore, the equivalent point estimation methods and the influence on tracking performance are studied and analysed in this paper. Based on the principle of radar measuring, the theoretical basis of classical equivalent point estimation algorithms, such as the strongest point, averaged point, centroid point and geometric centre, is combed. Furthermore, in view of the problems that the above methods fail to make full use of the structural information of the target group and are susceptible to non-ideal factors, a maximum group likelihood estimation method is proposed (for convenience, the corresponding equivalent point is called MGLE point in this paper). The performances of the five methods are verified and analysed through simulation. On this basis, the adaptability of different algorithms is discussed.

The rest of the paper is arranged as follows: in Section II, the general process of target group tracking is first introduced, and on this basis, two important issues of group division and equivalent point estimation are discussed. The performance of group division is directly related to the accuracy of equivalent point estimation. Aiming at the problem of instability of traditional K-Means algorithm, an improved method based on nearest neighbour association (NNA) algorithm and measurements set rearrangement is proposed, which provides a unified premise for the research of equivalent point estimation. On this basis, the mathematical models of the five equivalent point estimation algorithms are derived, and their design ideas are explained from the perspective of radar detection. In Section III, the above algorithms are simulated and analysed, the tracking performances of the five equivalent points are also compared. Finally, in Section IV, the work of this paper is summarized and the main conclusions are given.

II. TRACKING OF LOW-ALTITUDE SMALL TARGET GROUPS

The basic theory and framework of multi-target and formation target tracking are mature. Referring to the relevant research results, the general framework of target tracking for groups with dynamic outlines is given in [25]. Its main structure is shown in Figure 1.

Compared with the traditional target tracking framework, the main difference lies in the additional module of group division (in this paper, the modules of group separation detection and group merge detection in the original reference are also included in the group division module). The main purpose is to determine whether the measurements belong to the same group. In view of the special problems of LSTG tracking, the module of equivalent point estimation is further introduced to the framework, so as to achieve the optimal selection of tracking point in different working situations.

A. GROUP DIVISION

In this section, a robust group division algorithm is first introduced. Then, the effects of group distribution on the division results and the computation complexity are discussed.

1) A NOVEL GROUP DIVISION METHOD WITH ROUND-NNA

In existing literatures, K-Means algorithm is usually used to implement group division [26]. However, this algorithm

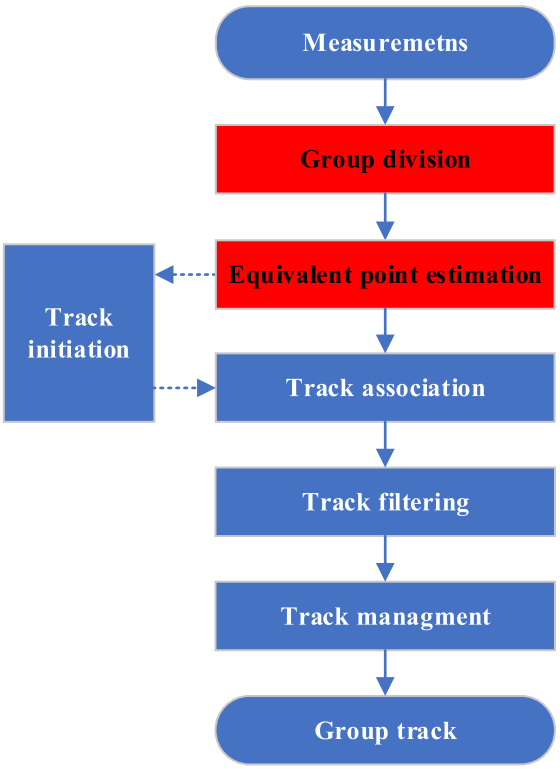

FIGURE 1. Diagram of LSTG tracking.

usually requires the number of groups in advance, and has the problem of slow convergence speed, which is not convenient for practical use. Many improvements have been made to the algorithm, but the selection of initial reference points is still not addressed. That is, the K-Means algorithm may lead to different group division results with different initial reference points. This will bring additional uncertainty to the performance evaluation of the subsequent equivalent point estimation algorithm.

Therefore, a robust group division algorithm based on NNA and measurements set rearrangement is presented in this section. For convenience, the algorithm is mentioned as Round-NNA in the following sections. The algorithm first determines the individual connection relationships with NNA, then rearranges the measurements set to avoid the influence of reference point selection. The algorithm achieves group division with connected domain analysis and the diagram is shown in Figure 2.

For a measurement set of N-point, the algorithm starts with the first member and associates it with other measurements. For all the associated measurements, they will be assigned the same group serial number and rearranged to the neighbour positions of the reference point. For the rearranged measurement set, the process of association and rearrangement is repeated. The division is implemented after all the measurements have been taken as the reference point.

Assuming that the measurements $\boldsymbol{M}_i$, $i = 1, 2 \cdots N$ of initial set $\boldsymbol{A}_1$ are labelled with the sequence they were acquired. Then the set can be expressed as:

$$\begin{array}{llllllll} Label: & 1 & 2 & 3 & 4 & 5 & \cdots & N \\ \boldsymbol{A}_1: & \boldsymbol{M}_1 & \boldsymbol{M}_2 & \boldsymbol{M}_3 & \boldsymbol{M}_4 & \boldsymbol{M}_5 & \cdots & \boldsymbol{M}_N \end{array} \quad (1)$$

The pseudo code of group division is given in Appendix and the detailed steps of a specific example are as follows:

Step 1): Take the first measurement $\boldsymbol{M}_1$ as the reference point, set the total group number $k = 1$ and the initial group number $g_1 = 1$, $g_i = 0$ for each measurement:

$$\begin{array}{llllllll} Label: & 1 & 2 & 3 & 4 & 5 & \cdots & N \\ \boldsymbol{A}_1: & \boldsymbol{M}_1 & \boldsymbol{M}_2 & \boldsymbol{M}_3 & \boldsymbol{M}_4 & \boldsymbol{M}_5 & \cdots & \boldsymbol{M}_N \\ g_i: & 1 & 0 & 0 & 0 & 0 & \cdots & 0 \end{array} \quad (2)$$

Step 2): For the measurements whose $Label = 2 \cdots N$, if $|\boldsymbol{M}_1 - \boldsymbol{M}_i| < Thr$ is satisfied, set $g_i = g_r$ (where Thr is the association threshold, g_r is the group number of reference measurement, for step 1),$g_r = 1$).For a specific example, the set can be expressed as:

$$\begin{array}{llllllll} Label: & 1 & 2 & 3 & 4 & 5 & \cdots & N \\ \boldsymbol{A}_1: & \boldsymbol{M}_1 & \boldsymbol{M}_2 & \boldsymbol{M}_3 & \boldsymbol{M}_4 & \boldsymbol{M}_5 & \cdots & \boldsymbol{M}_N \\ g_i: & 1 & 0 & 1 & 0 & 0 & \cdots & 0 \end{array} \quad (3)$$

To determine the association threshold, we can sort the measurements by distance and calculate the distance difference between adjacent points. Then the association threshold can be set as γ times the average value of the distance differences ($\gamma = 3$ in the simulation sections).

Step 3): Update $\boldsymbol{A}_1$ by rearranging the measurements whose group numbers are 1 to the front of the set, while other measurements are back shifted. Then the rearranged set $\boldsymbol{A}_2$ can be expressed as:

$$\begin{array}{llllllll} Label: & 1 & 2 & 3 & 4 & 5 & \cdots & N \\ \boldsymbol{A}_2: & \boldsymbol{M}_1 & \boldsymbol{M}_3 & \boldsymbol{M}_2 & \boldsymbol{M}_4 & \boldsymbol{M}_5 & \cdots & \boldsymbol{M}_N \\ g_i: & 1 & 1 & 0 & 0 & 0 & \cdots & 0 \end{array} \quad (4)$$

Step 4): Take the second measurement in $\boldsymbol{A}_2$ ($\boldsymbol{M}_3$ for the above example) as the new reference measurement and repeat step 2) - step 3) with measurements corresponding to $Label = 3, \cdots N$, the updated set is recorded as $\boldsymbol{A}_3$ (assuming that $\boldsymbol{A}_3$ is just the same with $\boldsymbol{A}_2$ in the example, i.e. none measurement is associated for $Label = 3, \cdots N$);

Step 5): Take the third measurement in $\boldsymbol{A}_3$ ($\boldsymbol{M}_2$ for the above example) as the new reference measurement. Since $g_3 = 0$, which means the measurement belongs to a new group. Set $k = 2, g_3 = 2$ and then repeat step 2)-step 3) with measurements corresponding to $Label = 4, \cdots N$,then the updated set $\boldsymbol{A}_4$ can be expressed as(assuming that $\boldsymbol{M}_4$ can be associated in this step):

$$\begin{array}{llllllll} Label: & 1 & 2 & 3 & 4 & 5 & \cdots & N \\ \boldsymbol{A}_4: & \boldsymbol{M}_1 & \boldsymbol{M}_3 & \boldsymbol{M}_2 & \boldsymbol{M}_4 & \boldsymbol{M}_5 & \cdots & \boldsymbol{M}_N \\ g_i: & 1 & 1 & 2 & 2 & 0 & \cdots & 0 \end{array} \quad (5)$$

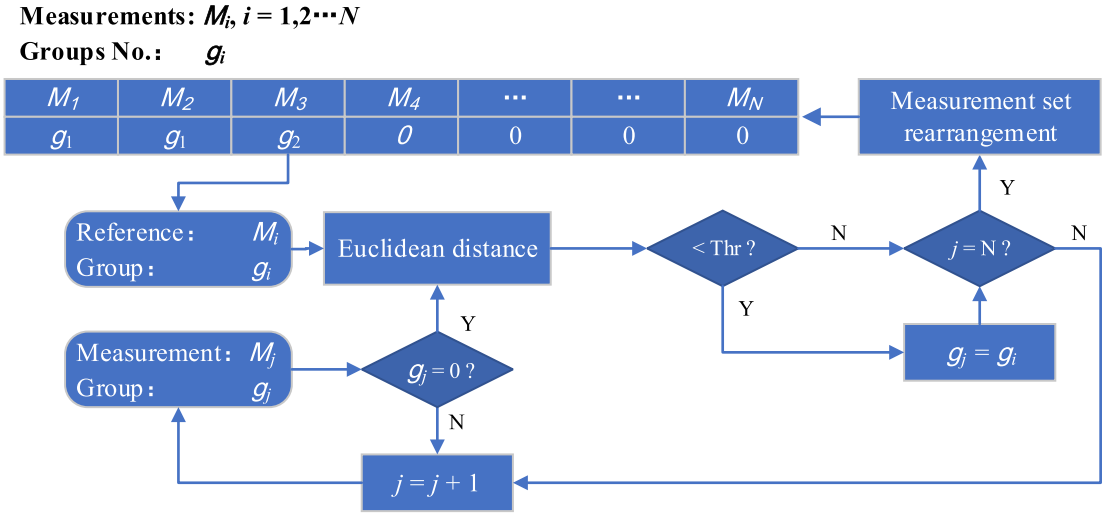

FIGURE 2. Diagram of robust group division algorithm.

Similar steps are then conducted for the rest measurements. The general process can be summarized that for the nth loop, take the nth measurement in $\boldsymbol{A}_n$ as the reference measurement:

1) If $g_n \neq 0$, it means the reference measurement has been divided into a certain group. Then step 2)- step 3) is directly repeated with measurements corresponding to $Label = n + 1, \cdots N$;
2) If $g_n = 0$, it means the reference measurement belongs to a new group. Then set $k = k + 1$, $g_n = k$ and repeat step 2)- step 3) with measurements corresponding to $Label = n + 1, \cdots N$;

With N-1 loops, the measurement can be divided successfully.

2) PERFORMANCE ANALYSIS

The performance of the group division algorithms can be evaluated from two aspects, i.e. the correctness of the results and the computation complexity. For the traditional K-Means algorithm, the group division result is related to the selection of reference point. Since the measurements are not labelled, it is difficult to select the ′optimal′ reference point. However, for the proposed algorithm, the group division result has little relationship with the selection of reference point (as can be seen from the simulations in Section III), so we simply choose the first measurement as the reference point in the simulation.

On the other hand, the distribution of the group outline (rather than the selection of reference point) may affect the calculation complexity of the proposed method.Since the group outline will change all the time, the calculation complexity is not fixed. The upper and lower bounds of computation complexity can be given for two extreme distribution types shown in Figure 3. For an N-member measurement set, the computational complexity are $(N-1)!\Delta$ for linear distribution (Figure 3a) and $(N-1)\,\Delta$ for stellate distribution (Figure 3b), respectively, where Δ means the unit computational complexity of association between a pair measurements (the association process repeats N times for linear distribution, while only once for stellate distribution).

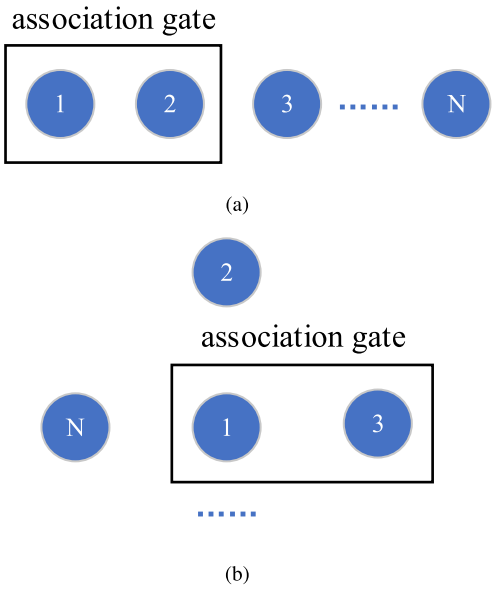

FIGURE 3. Group division under different set distribution. (a) linear distribution, (b) stellate distribution

B. EQUIVALENT POINT ESTIMATION

In this section, the theoretical basis of four classical equivalent point estimation algorithms, i.e., the strongest point, averaged point, centroid point and geometric centre, is combed first. Then, a maximum group likelihood estimation method is proposed. Aiming at the problem of large computation, the corresponding engineering implementation is also discussed.

1) CLASSICAL METHODS

a: TRACKING THE STRONGEST POINT

For narrowband radar systems with relatively low range resolution, the strongest point is usually selected for target measuring and tracking. It is assumed that the measurement set can be expressed as:

$$\varsigma_n = \{(\boldsymbol{Z}_i, a_i) \,|i = 1, 2 \cdots N\} \tag{6}$$

where $\boldsymbol{Z}_i$ is the target measurement, generally including range distance, azimuth and elevation angles information, and a_i is the corresponding magnitude of the target.

Based on the strongest point tracking principle, the equivalent point can be expressed as:

$$\boldsymbol{Z}_0 = \boldsymbol{Z}_k, \;\; k = \max_i \{a_i\} \tag{7}$$

However, with the improvement of radar resolution, the traditional point targets become extended targets, or indistinguishable targets become group targets that are individually distinguishable. Therefore, the strongest point is no longer used in modern high-resolution radar target tracking.

b: TRACKING THE AVERAGED POINT

Assuming that the group members are independently and identically distributed (i.i.d.), based on the central limit theorem, they can be modelled as Gaussian distribution with tracking point $\boldsymbol{Z}_0$ as the mean. Then, the joint probability density function (PDF) can be expressed as:

$$H = \prod_i \frac{1}{\sqrt{2\pi\sigma^2}} \exp\left[-\frac{(\boldsymbol{Z}_i - \boldsymbol{Z}_0)^2}{2\sigma^2}\right] \tag{8}$$

where σ^2 is distribution variance.

The corresponding logarithmic likelihood function is:

$$\begin{aligned} \eta &= \ln H \\ &= -\ln\sqrt{2\pi\sigma^2} - \frac{1}{2\sigma^2}\sum_i (\boldsymbol{Z}_i - \boldsymbol{Z}_0)^2 \end{aligned} \tag{9}$$

Ignoring the constant $-\ln\sqrt{2\pi\sigma^2}$, then the tracking point can be obtained with maximum likelihood estimation (MLE). The analytic expression is as follows:

$$\begin{aligned} \max_{z_0} \eta &= \min_{z_0} \sum_i (\boldsymbol{Z}_i - \boldsymbol{Z}_0)^2 \\ \Rightarrow \boldsymbol{Z}_0 &= \frac{1}{N}\sum_i \boldsymbol{Z}_i \end{aligned} \tag{10}$$

That is, average all the member measurements.

c: TRACKING THE CENTROID POINT

Furthermore, according to the theory of radar measuring, the accuracy of target measurement is related to signal to noise ratio (SNR). Therefore, by considering the SNR differences, Equation (8) can be rewritten as follows:

$$H = \prod_i \frac{1}{\sqrt{2\pi\sigma_i^2}} \exp\left[-\frac{(\boldsymbol{Z}_i - \boldsymbol{Z}_0)^2}{2\sigma_i^2}\right] \tag{11}$$

where σ_i^2 is distribution variance of measurement $\boldsymbol{Z}_i$.

The corresponding logarithmic likelihood function is:

$$\begin{aligned} \eta &= \ln H \\ &= -\sum_i \ln\sqrt{2\pi\sigma_i^2} - \sum_i \frac{(\boldsymbol{Z}_i - \boldsymbol{Z}_0)^2}{2\sigma_i^2} \end{aligned} \tag{12}$$

Then the maximum likelihood estimation is:

$$\boldsymbol{Z}_0 = \frac{\sum_i \frac{\boldsymbol{Z}_i}{\sigma_i^2}}{\sum_i \frac{1}{\sigma_i^2}} \tag{13}$$

Furthermore, we have:

$$\frac{1}{\sigma_i^2} \propto SNR = \frac{a_i^2}{\sigma_n^2} \tag{14}$$

where a_i is the amplitude of $\boldsymbol{Z}_i$,σ_n^2 is the noise power.

By taking (14) into (13), the following result can be obtained:

$$\boldsymbol{Z}_0 = \frac{\sum_i a_i^2 \boldsymbol{Z}_i}{\sum_i a_i^2} \tag{15}$$

It can be concluded that the averaged point and centroid point are essentially maximum likelihood estimates of measurement set under the assumption of Gaussian distribution. The former considers uniform measurement accuracy, while the latter considers the differences of measurement accuracy under different SNRs.

d: TRACKING THE GEOMETRIC CENTRE

Assuming that the obtained radar measurements are recorded as:

$$\boldsymbol{Z}_i = \begin{bmatrix} r_i & \alpha_i & \beta_i \end{bmatrix}^T, \quad i = 1, 2, \cdots M \tag{16}$$

where r_i, α_i, β_i are the range, azimuth and elevation angles of the ith measurement respectively.

The geometric centre of the measurement set can then expressed as:

$$\boldsymbol{Z}_i = \begin{bmatrix} r_i & \alpha_i & \beta_i \end{bmatrix}^T = \frac{1}{2}\begin{bmatrix} \min(\boldsymbol{r}) + \max(\boldsymbol{r}) \\ \min(\boldsymbol{\alpha}) + \max(\boldsymbol{\alpha}) \\ \min(\boldsymbol{\beta}) + \max(\boldsymbol{\beta}) \end{bmatrix} \tag{17}$$

where $\min(\cdot)$ and $\max(\cdot)$ are functions to estimate the minimum and maximum value of a set, respectively.

This method does not require any prior knowledge of the group structure, nor does it involve the magnitude information of member measurement.

2) NOVEL METHOD BASED ON MGLE

The classical methods did not consider the group structure information. Hence, the performance may degrade with the change of member status and environments. To address these issues, a novel method based on maximum group likelihood estimation (MGLE) is proposed in this section. By considering the association of group members to group measurements,

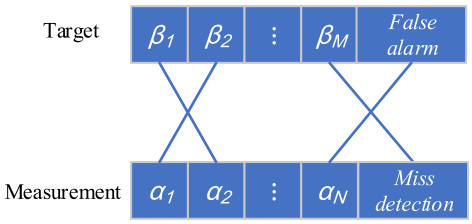

FIGURE 4. Typical association between measurements and group members.

the maximum likelihood function is built to describe the group structural information. On this basis, the optimal point is estimated.

Assuming that the target group is composed of M members whose true locations are:

$$\boldsymbol{\beta} = \left[\beta_1 \ \beta_2 \ \cdots \ \beta_M\right] \tag{18}$$

The measurement set of the current frame is:

$$\boldsymbol{\alpha} = \left[\alpha_1 \ \alpha_2 \ \cdots \ \alpha_N\right] \tag{19}$$

Considering of the possibility of false alarms and missed detections, the measurement number N is not equal to the target number M in general. The purpose of equivalent point estimation is to find an optimal tracking point from multiple scattering points, which need not be a specific target scatterer, but the point β_0 needs to satisfy the following characteristics:

1) The group motion can be correctly reflected and the tracking error should be as small as possible.
2) The point β_0 is stable in the group.

The relationship between the tracking point and the members of the target group can be modelled as follows:

$$\beta_i = \beta_0 + \tilde{\beta}_i, \quad i = 1, 2 \cdots M \tag{20}$$

where $\tilde{\beta}_i$ the position deviation of the ith member.

Assuming that the measurement α_j generates from the ith member, and then we have:

$$\alpha_j = \beta_i + n_j, \quad j = 1, 2 \cdots N \tag{21}$$

where n_j is the measurement noise obeys the standard Gaussian distribution $\mathcal{N}\left(0, \sigma^2\right)$.

As shown in Figure 4, a possible association between measurement set $\boldsymbol{\alpha}$ and target group $\boldsymbol{\beta}$ constitutes an observational event A_k (more than one measurements may be false alarms and more than one group member may be miss detected. But for the real measurements, their connections should be mutually exclusive, i.e., one measurement connects to only one member in an event). The joint PDF of event A_k can be expressed as:

$$p\left(A_k\right) = \prod_m p_m\left(\alpha_j|\beta_i\right) \cdot P_c \tag{22}$$

where $p_m\left(\alpha_j|\beta_i\right)$ represents the PDF of the mth connection in event A_k, since all the members of measurement set $\boldsymbol{\alpha}$ and target group $\boldsymbol{\beta}$ should be connected,$m \in [1, \max(M, N)]$; P_c represents the probability of occurrence of a specific connection, it can be defined as:

$$P_c = \begin{cases} P_{fa}, & \alpha_j \text{ is a false alarm} \\ 1 - P_d, & \beta_i \text{ is loss detection} \\ P_d, & \text{else} \end{cases} \tag{23}$$

For the specific connection between α_j and β_i, the PDF can be written as follows by combining (20) and (21):

$$\begin{aligned} p\left(\alpha_j|\beta_i\right) &= \frac{1}{\sqrt{2\pi\sigma^2}} \exp\left[-\frac{\left(\alpha_j - \beta_i\right)^2}{2\sigma^2}\right] \\ &= \frac{1}{\sqrt{2\pi\sigma^2}} \exp\left[-\frac{\left(\alpha_j - \beta_0 - \tilde{\beta}_i\right)^2}{2\sigma^2}\right] \end{aligned} \tag{24}$$

For the convenience of analysis, we assume that the measurements have the same noise variance. Then substituting (24) into (22), the logarithm likelihood function of event A_k can be expressed as:

$$L\left(A_k\right) = C_k - \frac{1}{2\sigma^2} \sum_m \left(\alpha_j - \beta_0 - \tilde{\beta}_i\right)_m^2 \tag{25}$$

where C_k is a constant which can be expressed as:

$$C_k = \ln\left[\left(\frac{P_d}{\sqrt{2\pi\sigma^2}}\right)^n (1 - P_d)^{M-n} P_{fa}^{N-n}\right] \tag{26}$$

where n is the number of non-false alarms from group members.

For all possible connections between measurements $\boldsymbol{\alpha}$ and target group $\boldsymbol{\beta}$, we can obtain the events set:

$$\boldsymbol{A} = \left[A_1 \ A_2 \ \cdots \ A_K\right] \tag{27}$$

The likelihood function of the set is the sum of all the sub-event likelihood functions:

$$L\left(\boldsymbol{A}\right) = \sum_{i=1}^{K} L\left(A_k\right) \tag{28}$$

The maximum likelihood solution can be achieved:

$$\hat{\beta}_0 = \arg\max_{\beta_0} L\left(\boldsymbol{A}|\beta_0\right) \tag{29}$$

When implementing the algorithm, the key step is to build the events A_k, which is essentially determining the association between measurements and target members.

For a target group contains M members and a set contains N measurements, ignoring the situations of miss detections and false alarms, there are M connection selections for the first measurement. After the first measurement is connected, there are $M-1$ connection selections for the second measurement, and so on. For all the N measurements, there are totally $M\,(M-1)\cdots(M-N+1)$ possible connections, which mean there are about 3.63 million possible connections for the case of $M = N = 10$. The calculation is so huge that it is almost impossible to be implemented in engineering uses. Therefore, it is necessary to explore efficient computing methods.

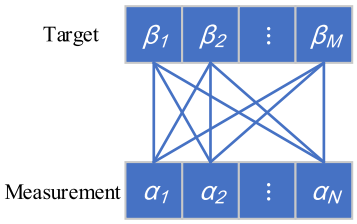

FIGURE 5. Full connection between measurements and group members.

For the specific the connection between α_j and β_i, the likelihood function is:

$$L_{ij} = \frac{1}{2\sigma^2}\left(\alpha_j - \beta_0 - \tilde{\beta}_i\right)^2 \tag{30}$$

In calculating the PDF of $\boldsymbol{A}$, Equation (30) will be accumulated for $K = (M-1)\cdots(M-N+2)$ times. Since the subscripts i and j can take any value from 1 to N and 1 to M, respectively. The group likelihood function is equivalent to K times the full connections (as shown in Figure 5.) between $\boldsymbol{\alpha}$ and $\boldsymbol{\beta}$. Therefore, for the same case of 10 targets and 10 measurements, it requires only 100 connections.

In case of false alarms or miss detections, Assuming that $\alpha_k(\beta_k)$ is a false alarm (miss detected), the likelihood function of event set can be expressed as:

$$\begin{aligned} L_{\alpha_k=fa} &= K[\![\boldsymbol{\alpha} \sim \boldsymbol{\beta}]\!] - \sum_{k=1}^{N}[\![\alpha_k \sim \boldsymbol{\beta}]\!] \\ &= (K-1)\,[\![\boldsymbol{\alpha} \sim \boldsymbol{\beta}]\!] \end{aligned} \tag{31}$$

where $[\![\boldsymbol{\alpha} \sim \boldsymbol{\beta}]\!]$ means likelihood function of the full connection between $\boldsymbol{\alpha}$ and $\boldsymbol{\beta}$.

It is not difficult to prove that the likelihood function for the case of l false alarms can be expressed as $(K-l!)\,[\![\boldsymbol{\alpha} \sim \boldsymbol{\beta}]\!]$. Therefore, the likelihood function of the whole group events can be expressed as multiple of full connection:

$$L(\boldsymbol{A}) = N_0[\![\boldsymbol{\alpha} \sim \boldsymbol{\beta}]\!] \tag{32}$$

where N_0 is a constant. This coefficient does not affect the final estimation result, so optimal estimation of the event set can be obtained by directly optimizing the full connection likelihood function.

III. SIMULATIONS AND ANALYSIS

A. SCENES AND PARAMETERS

Two situations are considered in this section to verify the performance of the above group tracking methods. The motion transition of the group member is defined by Couzin *et al.* model which is usually used for swarm behaviour modelling of birds, fishes, etc [27]. The model assumes that the members move with a fixed rate v, and only considers the changes of the position and direction of the members. Recording the spatial position and motion direction at time t of the ith member as $\vec{r}_i(t)$ and $\vec{\theta}_i(t)$, respectively, then the target motion state at time $t+\Delta t$ can be expressed as:

$$\begin{aligned} \vec{\theta}_i(t+\Delta t) &= rand\left[\vec{d}_i(t+\Delta t)\right] \\ \vec{r}_i(t+\Delta t) &= \vec{r}_i(t) + \vec{\theta}_i(t+\Delta t)\,v\Delta t \end{aligned} \tag{33}$$

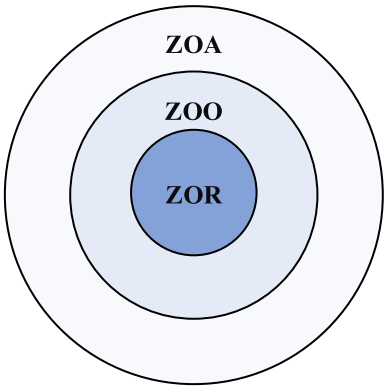

FIGURE 6. Interaction areas of Couzin model.

TABLE 1. Simulation parameters.

Variables	Values
Group number	2
Number of group member	50
Velocity	10 m/s
Initial group radius	10 m
Initial centre of Group1	(100 m, 100 m)
Initial centre of Group2	(200 m, 200 m)
Neighbourhood range	50 m
Update rate	0.1 s
Detection rate	0.9
False alarm rate	10^{-6}

where $\vec{d}_i(t+\Delta t)$ means the expected direction at $t+\Delta t$, *rand* $[\cdot]$ is random perturbations.

According to the SAC (separation, alignment and cohesion) rules [28], the Couzin model divides the perceptual regions of individuals into three zones, i.e. zone of repulsion (ZOR), zone of orientation (ZOO) and zone of attraction (ZOA) (as shown in Figure 6).

Let $N_i^{zor}, N_i^{zoa}, N_i^{zoo}$ represent the target set in corresponding zones, then the motion direction update can be conducted with the following equations:

$$\vec{d}_i(t+\Delta t) = \begin{cases} -\sum\limits_{j\in N_i^{zor}} \dfrac{\vec{r}_j(t)-\vec{r}_i(t)}{\left\|\vec{r}_j(t)-\vec{r}_i(t)\right\|}, & N_i^{zor} \neq \emptyset \\ \sum\limits_{j\in N_i^{zoa}} \dfrac{\vec{r}_j(t)-\vec{r}_i(t)}{\left\|\vec{r}_j(t)-\vec{r}_i(t)\right\|} \\ +\sum\limits_{j\in N_i^{zoo}} \dfrac{\vec{\theta}_j(t)}{\left\|\vec{\theta}_j(t)\right\|}, & N_i^{zor} = \emptyset \end{cases} \tag{34}$$

The main parameters used in the simulation are shown in Table 1.

B. ANALYSIS OF GROUP DIVISION

In order to investigate the effects of reference point selection on the group division performance, we first consider only one group with 100 measurements, whose positions follow the Gaussian distribution of (200m, 200m) as the centre and standard deviation 20m. In the group division process, each measurement is taken as the reference point in turn, and the association threshold is set to 100m. The ranges of

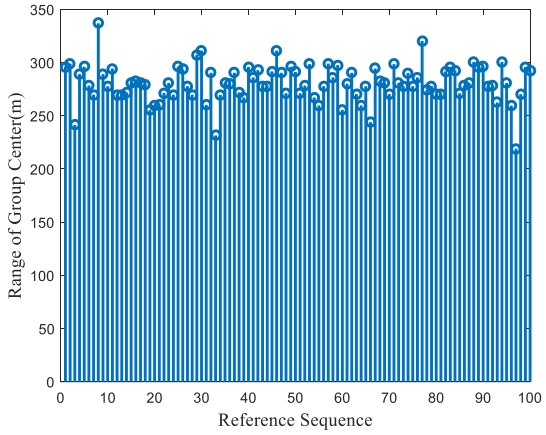

(a) ranges of group centre with K-Means algorithm

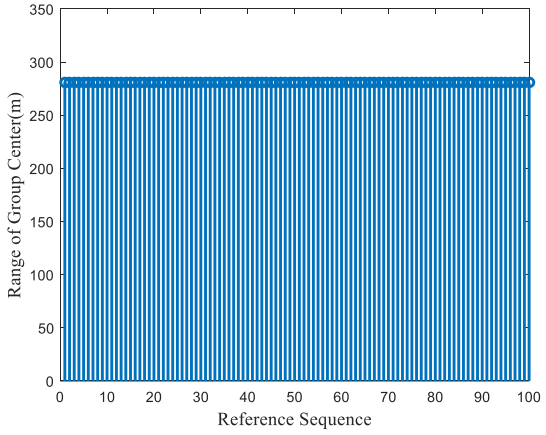

(b) ranges of group centre with Round-NNA algorithm

FIGURE 7. Effects of reference point selection on the group division performance.

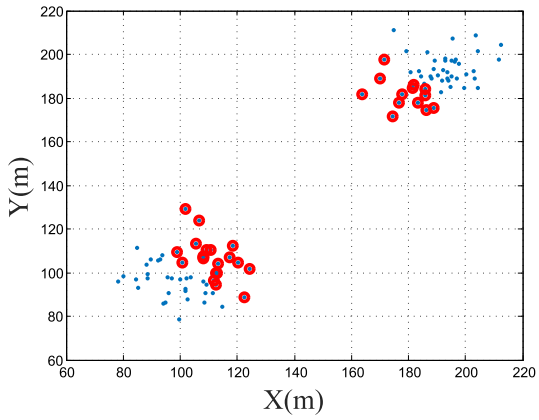

(a) reference point in error division

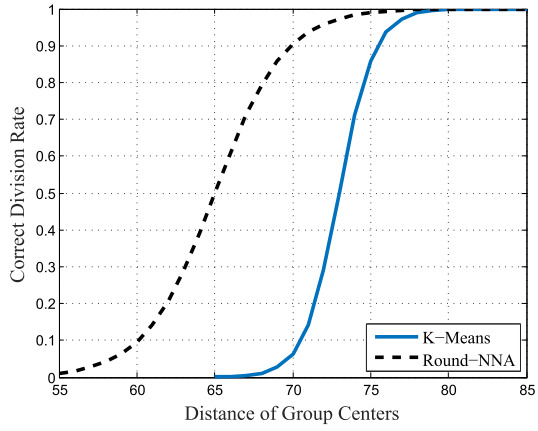

(b) performance under different group distances

FIGURE 8. Performance of group division.

group centre after division are calculated with the following equation and shown as Figure 7, in which the x axis (reference sequence) means the series number of the measurement in the measurement set.

$$x_0 = \frac{1}{N}\sum_i x_i$$
$$y_0 = \frac{1}{N}\sum_i y_i$$
$$R_0 = \sqrt{{x_0}^2 + {y_0}^2} \tag{35}$$

where x_i and y_i are the coordinates of the ith member of the group.

It can be seen that for the K-Means algorithm, the range of the group centre fluctuates significantly (peak to peak value 117m), while the centre range of the Round-NNA algorithm are much more stable. Hence it can be indicated that the selection of reference points has little effect on the group division results with Round-NNA algorithm.

Furthermore, for the two target groups in Table 1, the reference point of error division (with K-Means algorithm) is shown in the red circle in Figure 8(a). It can be seen that the error division occurs when the reference point is occasionally located between the two groups, in which case the division threshold should be reduced. However, since the location of the reference point cannot be known a prior in practice, which means the division threshold cannot be optimized a prior either. For the proposed algorithm, there is no such problem. The target groups can be divided correctly for any reference point. For the target groups with different distances, the true groups are recorded and compared with the group division results, then the correct division probability of the two algorithms is evaluated and shown in Figure 8(b). It can be seen that the proposed method can achieve more stable group division performance at a smaller group distance.

C. ANALYSIS OF EQUIVALENT POINT ESTIMATION

1) GROUP TRACKING WITH DIFFERENT EQUIVALENT POINTS

Two scenes of different complexity are considered in this section. The tracking process is first simulated, and then the range accuracies of the tracks are evaluated.

a: CASE 1: SIMPLE SCENE WITH TWO GROUPS

In this section, a simple scene with two groups is considered. The range-azimuth and time-range changing of each

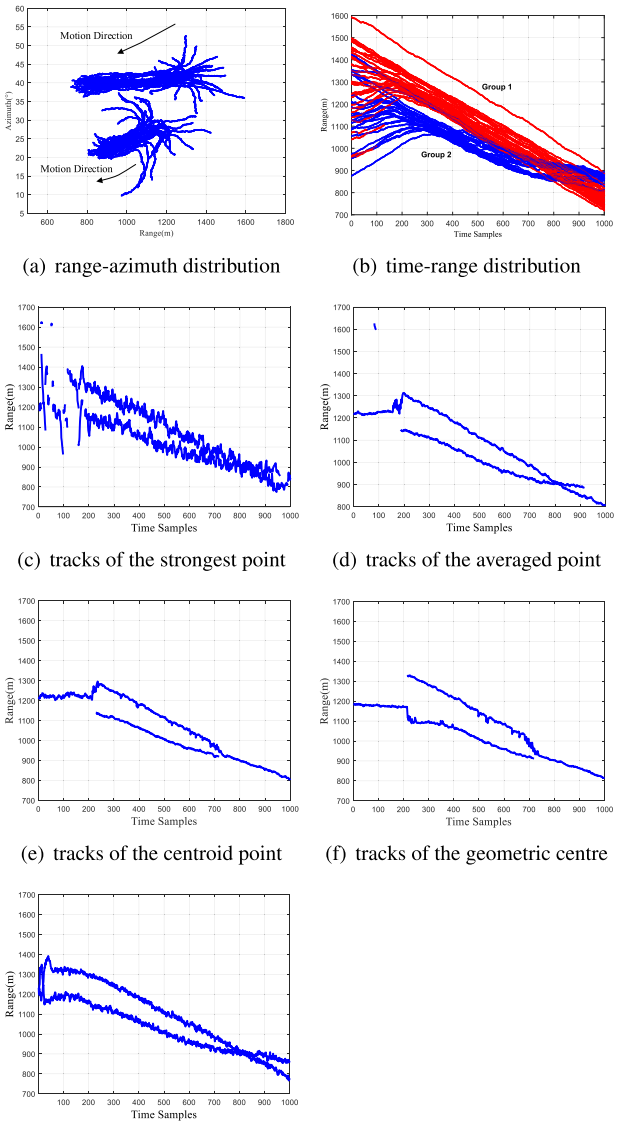

(a) range-azimuth distribution (b) time-range distribution

(c) tracks of the strongest point (d) tracks of the averaged point

(e) tracks of the centroid point (f) tracks of the geometric centre

(g) tracks of the MGLE point

FIGURE 9. **Group Tracking Results of simple scene.**

group member during the simulation period are shown in Figure 9(a) and (b), respectively. In Figure 9(b), the plots indicate the ranges of the individual targets to the radar and the different colours indicate different target groups. The group members first distribute randomly in a large area, then quickly gather and form two sub target groups, and finally move separately. Due to the occlusion between group members and the performance of detection algorithm, the number of measurements obtained at each time sampling duration is not necessarily equal to the number of group members, that is, there may be miss detections and false alarms. It can be seen that, a target group shows a unified overall movement trend, but at the same time, there are some track crossing, merging and moving away of local members. All these factors may lead to the variation of group structure, thus affecting the tracking performance.

Figure 9(c) shows the tracks of the strongest point. Because of the dramatically changes of the tracking point caused by individual attitude fluctuation, it can hardly form stable tracks when the two groups are not well separated. Besides, the tracks vibrate severely and the interruption occurs when two groups cross.

The tracking results of averaged point, centroid point and geometric centre are shown in Figure 9(d) - (f), respectively. The tracking performances of these three equivalent points are similar to each other on the whole. When two target groups are clearly separated, all of them can form stable tracks, while for the cases of group fusion and split, the tracks are all interrupted due to the position mutation of the equivalent points.

Figure 9(g) shows the track of the MGLE point proposed in this paper. It can be seen that the MGLE point has good adaptability to both the changes of internal structure and external contour of the group. It maintains continuous and stable group tracks in the situations of group crossing.

b: CASE 2: COMPLEX SCENE WITH MORE GROUPS AND INDIVIDUALS

To further evaluate the performance of the algorithm, we consider a more complex scene. In this scenario, the originally evenly distributed 150 targets were split into six groups and an individual target. Among them, group 1 to 4 consist of more members and have typical group structures; while group 5 and group 6 have fewer members(Figure 10(a) and (b)). It can be seen from Figure 10 (c)-(f) that as the complexity of the scene increases, the performance of traditional algorithms deteriorates obviously.

At the beginning of the simulation, the measurements have not yet formed clear groups. At this time, the strongest point (Figure 10 (c)) cannot form any stable track. Only when the groups are well separated, the continuous tracks are initiated and the tracks jitter severely. The tracking results of the averaged point (Figure 10 (d)), the centroid point (Figure 10 (e)) and the geometric center (Figure 10 (f)) are obviously better than that of the strongest points. But for group 3 and group 5, their tracking results do not accurately reflect the motion characteristics. The group 3 first moved slowly around 1000m. Later, due to the influence of group 2, its movement direction gradually became the same as that of group 2. And the group 5 always moves slowly around 900m. However, the above three methods incorrectly merged the measurements of group 5 and group 3, so the track of group 3 disappeared after the 600th frame and only the track of group 5 was retained.

For the proposed method, it can maintain continuous tracks for all the six groups and the individual target (Figure 10 (g)). Meanwhile, the tracking results correctly reflected the movement of each target (group). For the group 5, its track is always around 900m; while for the group 3, its track changes from being almost fixed to gradually approaching after the 600th frame, and its movement is similar to the track of group 2.

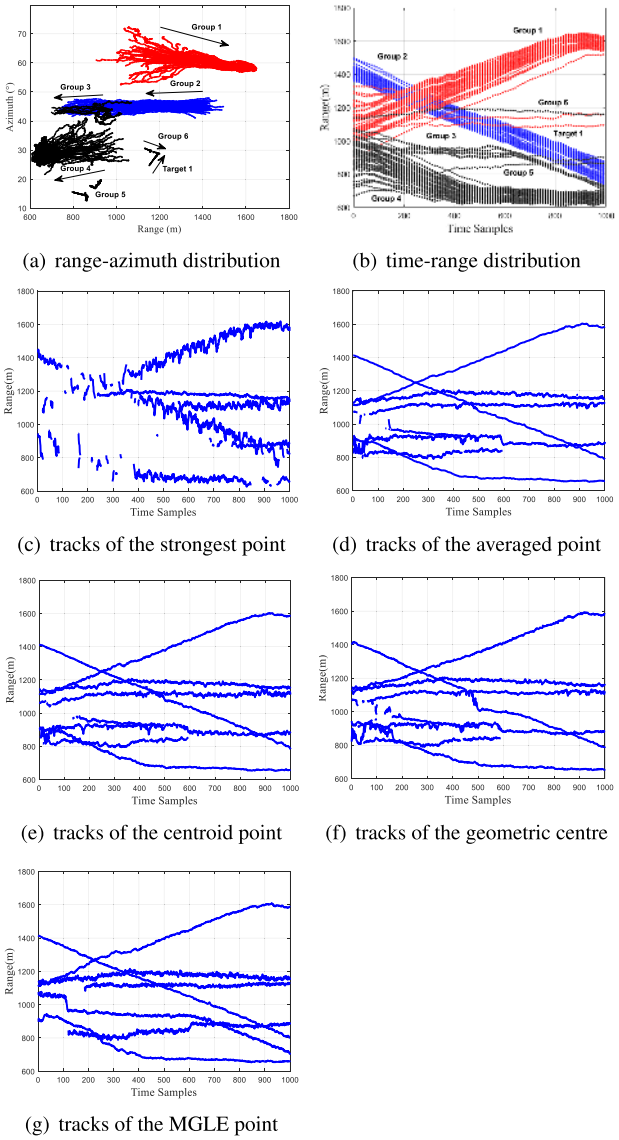

(a) range-azimuth distribution (b) time-range distribution

(c) tracks of the strongest point (d) tracks of the averaged point

(e) tracks of the centroid point (f) tracks of the geometric centre

(g) tracks of the MGLE point

FIGURE 10. Group Tracking Results of complex scene.

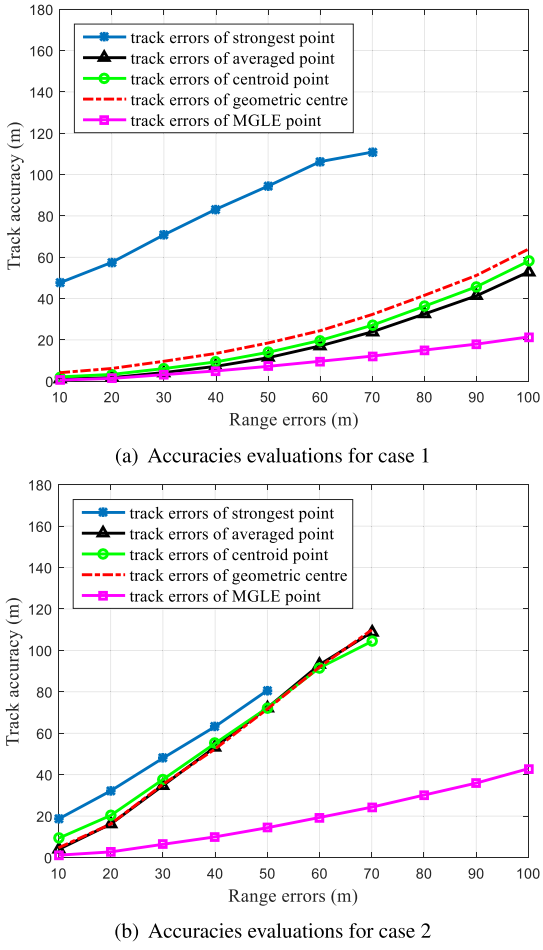

(a) Accuracies evaluations for case 1

(b) Accuracies evaluations for case 2

FIGURE 11. Tracking accuracies of different equivalent point.

2) PERFORMANCE EVALUATION

Because the change of group motion state is caused by the interaction between individuals, it is hard to define the real track. Therefore, a fourth-order differential method [29] is introduced, and on this basis, the tracking performance of different equivalent points is evaluated.

The fourth-order differential method considers that in a measurement set, the true value and the system errors are slowly-time-varying functions which can be represented by a polynomial; while the random error is a stationary process. The measurement sequence can be expressed as:

$$y_i = \sum_{j=1}^{P} A_{j-1} t_i^{j-1} + \xi_i \tag{36}$$

where P is the polynomial order, A_{j-1} is the polynomial coefficients, and ξ_i is random error.

Considering the slowly-varying characteristics of the true value and system errors, the random error can be calculated with P-order difference to the measurement sequence

$$\Delta^P y_i = \sum_{j=0}^{P} a_j y_{i+j} \tag{37}$$

where $a_j = (-1)^j C_P^j$.

Then the tracking accuracy, i.e. the root mean square (RMS) value of the random error, can be expressed as

$$\sigma = \sqrt{\frac{(P!)^2}{(2P)!} mean\left(\left(\Delta^P y_i\right)^2\right)} \tag{38}$$

To evaluate the algorithm performance, the track accuracy assessment method is designed as follows:

1) taking range measurements as an example, the standard deviation of its measurement error is increased from 10m to 100m.
2) in a simulation, when all the tracks in the scene are successfully tracked, the simulation is considered valid;
3) calculate the average accuracy of all tracks as the output of the accuracy assessment, where the accuracy of a

single track is still given by the Equation (38) in the paper;

4) for each error deviation, 50 repeated experiments are performed:
   a) when the success rate is greater than 90%, the average value of multiple accuracy evaluation results is calculated as the final output.
   b) otherwise the algorithm is regarded as failed.

For the two scenarios above, the track accuracy evaluation results are shown in Figure 11. It can be seen that:

1) The tracking accuracy of the strongest point is the lowest and the adaptability to the measurement error is also the smallest;
2) The tracking performances of the averaged point, centroid point and geometric centre are comparable. In the simple scenario, all of they can keep stable tracking; while in complex scenario, the success tracking rate decreases when the error is large;
3) For the proposed method, it has the lowest tracking error and the best tracking continuity. In the complex scenario, when the range measurement error is greater than 100m, the algorithm cannot track the target group. This is because that the measurement error at this time is larger than the distribution range of the group, hence the stable group structure cannot be maintained.

IV. CONCLUSION

Group division and equivalent point estimation are two important modules in group tracking. It is directly related to the performance of group centre tracking, as well as the accuracy of group outline estimation. For the former issues, the paper proposes a group division method based on improved nearest neighbour Association. Compared with the traditional K-means algorithm, it can avoid the division differences caused by the selection of reference points. For the latter, the paper analyses the mathematical basis of four traditional equivalent point estimation methods, and on this basis, proposes a maximum group likelihood equivalent point estimation method using group structure information. The simulation results show that MGLE point can keep a stable track with the none ideal factors of group fusion, group splitting or large measurement errors.

V. APPENDIX:PSEUDO CODE OF GROUP DIVISION

Input:

Measurement set:

$$\boldsymbol{A} = [\boldsymbol{M}_1 \quad \boldsymbol{M}_2 \quad \cdots \quad \boldsymbol{M}_N]$$

Initial group series of measurements:

$$\boldsymbol{G} : \{g_i = -1, i = 1, 2 \cdots N\}$$

Initial total number of groups:

$$G_0 = 0$$

for $i = 1$ to N

// Set the reference measurement and its group serial number

$\boldsymbol{X}_0 \leftarrow \boldsymbol{A}(i)$

if $g_i = -1$, then

$G_0 \leftarrow G_0 + 1$

$g_i \leftarrow G_0$

end if;

// Association of reference measurement and group member

for $j = i + 1$ to N

if $|\boldsymbol{X}_0 - \boldsymbol{A}(j)| < Thr$, then

$g_j \leftarrow G_0$

end if;

end for;

// Rearranging the measurement set and the group serial numbers

$\boldsymbol{Y}_1 \leftarrow \boldsymbol{A}(1 : i)$

$\boldsymbol{P}_1 \leftarrow \boldsymbol{G}(1 : i)$

$k_1 \leftarrow 0$

$k_2 \leftarrow 0$

for $j = i + 1$ to N

if $g_j = G_0$, then

$k_1 \leftarrow k_1 + 1$

$\boldsymbol{Y}_2(k_1) \leftarrow \boldsymbol{A}(j)$

$\boldsymbol{P}_2(k_1) \leftarrow \boldsymbol{G}(j)$

else

$k_2 \leftarrow k_2 + 1$

$\boldsymbol{Y}_3(k_2) \leftarrow \boldsymbol{A}(j)$

$\boldsymbol{P}_3(k_2) \leftarrow \boldsymbol{G}(j)$

end if;

end for;

$\boldsymbol{A} \leftarrow [\boldsymbol{Y}_1 \quad \boldsymbol{Y}_2 \quad \boldsymbol{Y}_3]$

$\boldsymbol{G} \leftarrow [\boldsymbol{P}_1 \quad \boldsymbol{P}_2 \quad \boldsymbol{P}_3]$

end for;

for $i = 1$ to G_0

Find measurements in $\boldsymbol{A}$ whose group serial number is i

Forming group $\boldsymbol{C}_i$ with these measurements

end for;

Output:

Divided measurement groups:

$$\boldsymbol{C}_i, i = 1, 2 \cdots G_0$$

REFERENCES

[1] M. Ponti, A. A. Chaves, F. R. Jorge, G. B. P. Costa, A. Colturato, and K. R. L. J. C. Branco, "Precision agriculture: Using low-cost systems to acquire low-altitude images," *IEEE Comput. Graph. Appl.*, vol. 36, no. 4, pp. 14–20, Jul. 2016.

[2] X. Liu, P. Chen, X. Tong, S. Liu, S. Liu, Z. Hong, L. Li, and K. Luan, "UAV-based low-altitude aerial photogrammetric application in mine areas measurement," in *Proc. 2nd Int. Workshop Earth Observ. Remote Sens. Appl.*, Shanghai, China, Jun. 2012, pp. 240–242.

[3] N. Lakshman, R. Raj, and Y. Mukkamala, "Bird strike analysis of jet engine fan blade," in *Proc. IEEE Aerosp. Conf.*, Big Sky, MT, USA, Mar. 2014, pp. 1–7.

[4] G. Galati, E. G. Piracci, and M. Ferri, "High resolution, millimeter-wave radar applications to airport safety," in *Proc. 8th Int. Conf. Ultrawideband Ultrashort Impulse Signals (UWBUSIS)*, Sep. 2016, pp. 21–26.

[5] H. Zhang, J. Xie, J. Shi, Z. Zhang, and X. Fu, "Sensor scheduling and resource allocation in distributed MIMO radar for joint target tracking and detection," *IEEE Access*, vol. 7, pp. 62387–62400, 2019.

[6] T. Wagner, R. Feger, and A. Stelzer, "Radar signal processing for jointly estimating tracks and micro-Doppler signatures," *IEEE Access*, vol. 5, pp. 1220–1238, 2017.
[7] A. Angelov, A. Robertson, and R. Murraysmith, "Practical classification of different moving targets using automotive radar and deep neural networks," *IET Radar, Sonar Navigat.*, vol. 12, no. 10, pp. 1082–1089, 2018.
[8] T. Cheng, S. Li, and J. Zhang, "Adaptive resource management in multiple targets tracking for co-located multiple input multiple output radar," *IET Radar, Sonar Navigat.*, vol. 12, no. 9, pp. 1038–1045, Sep. 2018.
[9] P. Wan, B. Hao, Z. Li, X. Ma, and Y. Zhao, "Accurate estimation the scanning cycle of the reconnaissance radar based on a single unmanned aerial vehicle," *IEEE Access*, vol. 5, pp. 22871–22879, 2017.
[10] G. Trajcevski and P. Scheuermann, "Targets and shapes tracking (advanced seminar)," in *Proc. 19th IEEE Int. Conf. Mobile Data Manage. (MDM)*, Jun. 2018, pp. 7–10.
[11] A. P. Frazier and J. A. Scott, "ATOMS-1: An algorithm for tracking of moving sets," Syst. Planning Corp., Arlington, VA, USA, Tech. Rep. ECOM-0510-4, AD-B015080L, 1976.
[12] S. S. Blackman, *Multiple-Target Tracking With Radar Applications*. Norwood, MA, USA: Artech House, 1986, pp. 204–205.
[13] O. E. Drummond, "Tracking clusters and extended objects with multiple sensors," in *Proc. Signal Data Process. Small Targets*, Oct. 1990, pp. 364–375.
[14] K. Granstrom and U. Orguner, "On spawning and combination of Extended/Group targets modeled with random matrices," *IEEE Trans. Signal Process.*, vol. 61, no. 3, pp. 678–692, Feb. 2013.
[15] G. Amadou, M. Lyudmila, and M. Simon, "Ground target group structure and state estimation with particle filtering," in *Proc. 11th Int. Conf. Inf. Fusion*, Cologne, Germany, Jun. 2008, pp. 1–8.
[16] M. Baum and U. D. Hanebeck, "Extended object tracking with random hypersurface models," *IEEE Trans. Aerosp. Electron. Syst.*, vol. 50, no. 1, pp. 149–159, Jan. 2014.
[17] M. Baum and D. Hanebeck, "Random hypersurface models for extended object tracking," in *Proc. IEEE Int. Symp. Signal Process. Inf. Technol. (ISSPIT)*, Ajman, United Arab Emirates, Dec. 2009, pp. 178–183.
[18] J. Lan and X. R. Li, "Tracking of extended object or target group using random matrix Part II: Irregular object," in *Proc. Int. Conf. Inf. Fusion*, Singapore, 2012, pp. 2185–2192.
[19] S. K. Pang, J. Li, and S. J. Godsill, "Detection and tracking of coordinated groups," *IEEE Trans. Aerosp. Electron. Syst.*, vol. 47, no. 1, pp. 472–502, Jan. 2011.
[20] A. Gning, L. Mihaylova, S. Maskell, S. K. Pang, and S. Godsill, "Group object structure and state estimation with evolving networks and Monte Carlo methods," *IEEE Trans. Signal Process.*, vol. 59, no. 4, pp. 1383–1396, Apr. 2011.
[21] K. Granstrom, A. Natale, P. Braca, G. Ludeno, and F. Serafino, "Gamma Gaussian inverse wishart probability hypothesis density for extended target tracking using X-Band marine radar data," *IEEE Trans. Geosci. Remote Sens.*, vol. 53, no. 12, pp. 6617–6631, Dec. 2015.
[22] J. W. Koch, "Bayesian approach to extended object and cluster tracking using random matrices," *IEEE Trans. Aerosp. Electron. Syst.*, vol. 44, no. 3, pp. 1042–1059, Jul. 2008.
[23] Z. Fu, P. Feng, F. Angelini, J. Chambers, and S. M. Naqvi, "Particle PHD filter based multiple human tracking using online group-structured dictionary learning," *IEEE Access*, vol. 6, pp. 14764–14778, 2018.
[24] L. Gan and G. Wang, "Tracking the splitting and combination of group target with δ -generalized labeled multi-Bernoulli filter," *IEEE Access*, vol. 7, pp. 81156–81176, 2019.
[25] W. D. Geng, Y. Q. Wang, and Z. H. Dong, *Group Target Tracking*. Beijing, China: National Defense Industry press, 2014, pp. 12–24.
[26] W. Chen, H. Liu, S. Hu, and H. Ning, "Group tracking of flock targets in low-altitude airspace," in *Proc. IEEE 9th Int. Symp. Parallel Distrib. Process. with Appl. Workshops*, May 2011, pp. 131–136.
[27] I. D. Couzin, J. Krause, R. James, G. D. Ruxton, and N. R. Franks, "Collective memory and spatial sorting in animal groups," *J. Theor. Biol.*, vol. 218, no. 1, pp. 1–11, Sep. 2002.
[28] I. Giardina, "Collective behavior in animal groups: Theoretical models and empirical studies," *HFSP J.*, vol. 2, no. 4, pp. 205–219, Sep. 2010.
[29] Y. X. Lou, *Radar Accuracy Analysis*, Beijing, China: National Defence Industry Press, China, 1979.

CHAO ZHOU was born in Jiangsu, China, in 1987. He received the B.S. degree in information engineering from Soochow University, in 2013, and the Ph.D. degree in information and communication engineering from the Beijing Institute of Technology (BIT), Beijing, China, in 2018. He is currently working as a Postdoctoral Researcher with the Radar Technology Research Laboratory, BIT. He has published over 20 articles in international journals and radar conferences. His research interests include radar detection and tracking algorithms, and radar ECCM technologies.

RUI WANG was born in Taiyuan, Shanxi, China, in 1985. He received the B.S. degree in information engineering and the Ph.D. degree in information and communication engineering from the Beijing Institute of Technology, Beijing, China, in 2009 and 2015, respectively. From 2012 to 2013, he was a Visiting Scholar with the Mullard Space and Science Laboratory, University College London, London, U.K. From 2015 to 2017, he was a Postdoctoral Researcher with the Department of Electronics Engineering, Tsinghua University, Beijing. Since 2018, he has been an Associate Professor with the School of Electronic Engineering, Beijing Institute of Technology. His research interests include bistatic synthetic aperture radar (SAR) imaging, stepped-frequency radar signal processing, ISAR imaging, and entomological radar signal processing to extract insect biological parameters. He was a recipient of the IEEE CIE International Radar Conference Excellent Paper Award, in 2011.

CHENG HU received the B.S. degree in electronic engineering from the National University of Defense Technology, in July 2003, and the Ph.D. degree in target detection and recognition from the Beijing Institute of Technology (BIT), in July 2009. He was a Visiting Research Associate with the University of Birmingham for 15 months, from 2006 to 2007. In September 2009, he joined with the School of Information and Electronics, BIT, where he has been a Full Professor, since 2014. He is currently a Full Professor, a Ph.D. Supervisor, and the Vice-Director of the Radar Research Laboratory, BIT. He has published over 60 SCI-indexed journal articles and over 100 conference papers. His main research interests include new concept synthetic aperture radar imaging and the biological detection radar systems and signal processing.